ferred between the S-registers and the ARU memory. The I/O Control Unit interferes with the Main Control Unit only when it reads an I/O-command from main control's program memory. One I/O command can move many bit-planes of data so this interference is minimized.

Companion Processor

A conventional computer manages data flow between MPP units, loads programs into the ACU, executes system-test and diagnostic routines, and provides program development facilities. This computer initially will be a DEC PDP-11/34. After system checkout, a DEC VAX 11/780 will assume the functions of the companion processor.

Staging Buffer

The MPP system will include a staging memory for buffering ARU data. This memory provides the "corner turning" function, which converts conventional byte-oriented data into the bit plane form needed by the ARU. The capacity of this memory will be 512 Kbytes when the MPP is delivered. It will be expandable to 16 Mbytes (using currently available memory chips) with a transfer rate to and from the ARU of 160 Mbytes/s. Later use of advanced memory chips will allow the capacity to increase to 64 Mbytes.

Software

System software for the MPP consists of program development software and diagnostic software. The program development software supports usage of the MPP's massive data processing capability while the diagnostics package supports checkout of the MPP system hardware. The user software interface to MPP will be via assembler language or Parallel Pascal. Parallel Pascal is an extention of standard Pascal which allows direct use of the MPP array architecture while programming in the high-level language. A user subroutine library will be provided.

Conclusion

Spatially parallel computers, such as the MPP, hold the promise of being the prevalent type of computer that will be used in making decisions based on real-time image inputs. Such on-line automatic decision making based on visual inputs is needed both for governmental and industrial uses. Future computers having over one million processing elements are envisioned. The MPP is an important initial step in the realization of computers that really can "see."

References

[1] Schaefer, D.H., "Massively Parallel Processing Systems for Space Application," *Proceedings of 2nd AIAA Computers in Aerospace Conference,* Oct. 1979, p. 284.

[2] Batcher, K.E., "Design of a Massively Parallel Processor," *IEEE Transactions on Computers,* Vol. C29, Sept. 1980, pp. 836-840.

AIAA 82-4130

Deadband Control System Limit Cycles Analyzed by Fourier Series

Franklin C. Loesch*
The Aerospace Corporation, El Segundo, Calif.

Introduction

THE limit cycles of a missile's post-boost deadband pneumatic attitude control system are analyzed by calculating the switching time delays of the real system relative to an ideal system in which the transfer function of each linear element is 1. These on and off delays are first derived by considering the geometric and timing relations between the missile's motion and the ideal switching lines in the missile's phase plane. The same delays are then calculated by representing the limit cycle rate vs time as a Fourier series; then deriving the deadband switch's input as another Fourier series in which the dynamic response of each linear element is accounted for. The limit cycle solution is obtained by a simple trial and interpolation method, which finds the maximum rate and duty fraction for which corresponding delays as calculated by both procedures are equal. Using 50 to 100 Fourier series terms, this method gives essentially exact results that agree with digital simulations within 1 to 2%. The accuracy of the method is easily assessed graphically, or by determining the changes in solution values as the number of Fourier terms and the size of the interpolation intervals are changed. Unequal solenoid valve on and off delays are accounted for easily. The method is limited to simple deadband systems for which the character of the limit cycle's rate time history is known beforehand. The method may become impractical for duty fractions less than about 1%, because the Fourier series may not accurately represent the system near the switching points with an acceptable number of terms.

Other methods for calculating limit cycle characteristics include Patapoff's,[1] which is restricted to small duty fraction cases for which all transients have essentially decayed prior to switch on. His method is not applicable to such cases as analyzed here, in which the off delay may even exceed the time to cross the deadband. Approximate methods include simple engineering estimates of the effective delays of the linear elements. It is shown here that the usual estimates of these delays result in overpredictions of duty fractions by 40 to 400%. The well-known describing function technique[2,3] is a complicated approximate method, which is not able to account for the unequal on and off valve delays, and which has no intrinsic accuracy assessment capability. It appears that with the availability of computers for which the Fourier series and trial computations are trivial, the Fourier series method is superior to the describing function method because it is essentially exact rather than approximate, its accuracy is easily assessed, it accounts for unequal valve delays without resort to Padé[3] approximations, and it appears to be simpler.

Phase Plane Delay/Rate/Duty Fraction Relations

Figure 1 shows one axis of the deadband system. The pneumatic thrusters impart a constant angular acceleration $\ddot{\theta}$. Throughout this Note, all angular rates except ω are made nondimensional by dividing by $\lambda\ddot{\theta}$, where λ is the rate gain, and all angles except ωt are normalized by dividing by $\lambda^2\ddot{\theta}$. For brevity, these divisors are omitted; so B stands for $B/\lambda^2\ddot{\theta}$, etc. Figure 2 shows the missile's symmetric limit cycle in the nondimensional phase plane. The lines with slope of -1 are the ideal switching lines; i.e., these would be the switching lines if the transfer functions of all linear elements in the system were 1. The real transfer functions are not 1; hence, the real switch off occurs at point 0′ rather than point 0. Nozzle 1 off occurs later than 0′, due to the valve off delay; it may occur at point 1, before, or at alternate point 1, after crossing the No. 2 ideal on line.

The total on time is $4\dot{\theta}_{max}$. The total drift time is $4(\theta_4/\dot{\theta}_{max})$. Using the phase plane parabola relation to replace θ_4 by θ_{max}, the limit cycle angular frequency ω and the duty fraction D are obtained:

$$(\omega\lambda/2\pi) = D/4\dot{\theta}_{max} \qquad D = \dot{\theta}^2_{max}/[\theta_{max} + (\dot{\theta}^2_{max}/2)] \quad (1)$$

The relevant points in Fig. 2 are determined by intersections or time differences as shown in Table 1.

By defining these intersections and time differences analytically, using the equations for the No. 1 parabola, the ideal switching lines and the drift lines, together with sym-

Received April 24, 1981; revision received Jan. 4, 1982.

*Senior Engineer, Payload Integration and Mission Operations Directorate.

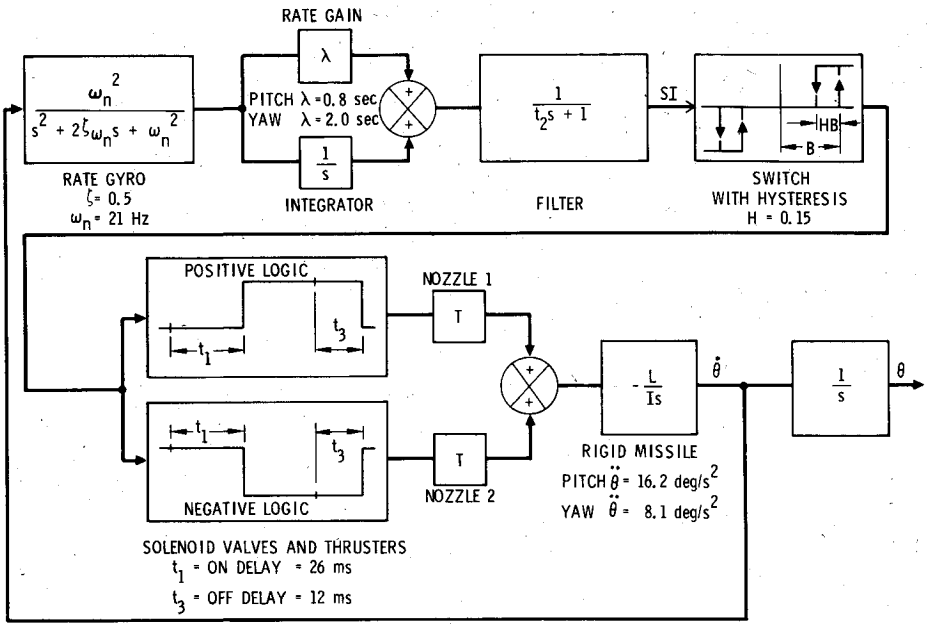

Fig. 1 Block diagram of deadband control system.

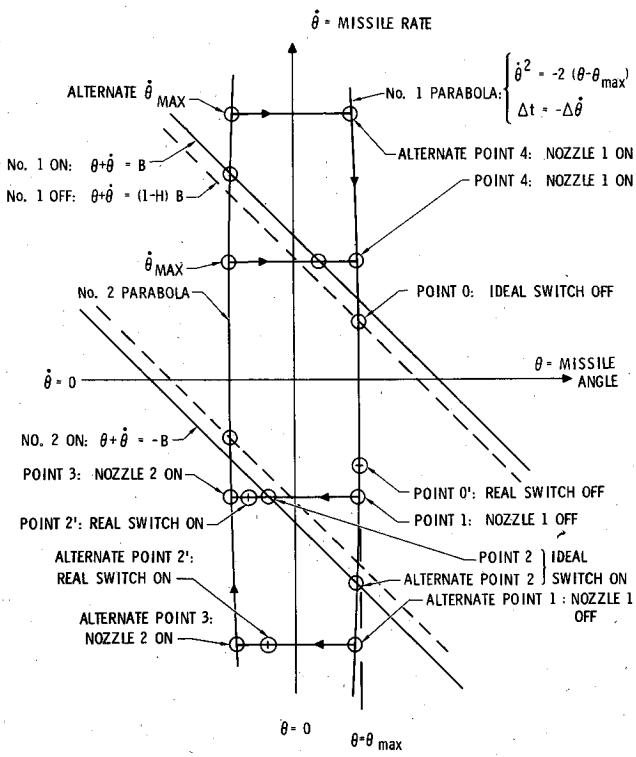

Fig. 2 Zero disturbance limit cycle—nondimensional phase plane.

Table 1 Phase plane points

Point	Intersection	Time difference
0	1 off and 1 parabola	...
1 or alternate 1	...	t_{off} after point 0
Alternate 2	2 on and 1 parabola	Δt_{DB} = time to cross deadband
2	2 on and point 1 rate	...
3	...	t_{on} after point 2
Alternate 3	...	t_{on} after alternate point 2

metry relations, a set of equations is obtained from which, by successive eliminations and manipulations, the following expressions for t_{off}, t_{on}, and Δt_{DB} are obtained.

$$t_{off}^2 - 2(1+\dot{\theta}_{max})t_{off} + 2[(1-H)B + \dot{\theta}_{max} - \dot{\theta}_{max}^2(1-D)/D] = 0$$

$$t_{on} = 1 + \dot{\theta}_{max}(1-D)/D - (B/\dot{\theta}_{max}) \qquad t_{off} \le \Delta t_{DB}$$

$$t_{on} = 2\dot{\theta}_{max}(1-D)D + t_{off} - \Delta t_{DB} \qquad t_{off} \ge \Delta t_{DB}$$

$$\Delta t_{DB} = [b - (b^2 - c)^{1/2}]^{1/2} \qquad b = 2(1 + 2\theta_{max} + HB)$$

$$c = [2(2-H)B]^2 \tag{2}$$

Time Plane Delay/Rate/Duty Fraction Relations

The limit cycle rate vs time is a periodic function with angular frequency ω. Define one cycle from $-\pi$ to $+\pi$ so that $\omega t = 0$ occurs in the middle of the drift from point 1 to 3. Supposing that the rate gyro and filter have transfer functions of 1, the switch input can be calculated by integrating and summing the rate and applying symmetry relations. The resulting ideal switch input, which is plotted in Fig. 3, is

$$SI/\dot{\theta}_{max} = -A/D - (B/D)\omega t - (C/D)(\omega t)^2 \qquad \text{nozzle 1 on}$$

$$SI/\dot{\theta}_{max} = -1 - (2\dot{\theta}_{max}/\pi D)\omega t \qquad \text{drift}$$

$$A = 1 + (\dot{\theta}_{max}(1-D)^2/2D) \qquad B = (2/\pi) + (2\dot{\theta}_{max}/\pi D)$$

$$C = 2\dot{\theta}_{max}/\pi^2 D \tag{3}$$

The missile's limit cycle rate is approximated by a Fourier series. The switch input for the real system is obtained easily by calculating sequentially: the gyro's response, the integrator's output considering symmetry requirements, the filter input and the filter's response.

$$\frac{SI}{\dot{\theta}_{max}} = \sum_{1}^{n} a_n G_n E_n \left[1 + \left(\frac{1}{n\lambda\omega}\right)^2\right]^{1/2} \cos(n\omega t - \phi_n - \beta_n - \psi_n)$$

$$a_n = -(8/n^2\pi^2 D)\sin(n\pi/2)\sin(n\pi D/2)$$

$$\beta_n = \tan^{-1}(1/n\lambda\omega) \qquad 0 \le \beta_n \le \pi \tag{4}$$

Table 2 Limit cycle solutions and estimates

	Duty fraction	Gyro-filter off delay, ms	Gyro-filter on delay, ms	Max rate, deg/s	Max angle, deg	Frequency, Hz
Case 1[a]—Pitch: $B=0.5$ deg, $t_2=187$ ms						
Fourier series	0.307	69.6	264	1.00	0.17	1.25
Sinusoidal estimate	0.471	122	122	1.32	0.18	1.44
Case 2[a]—Yaw: $B=0.65$ deg, $t_2=187$ ms						
Fourier series	0.107	55.0	295	0.32	0.11	0.67
Sinusoidal estimate	0.428	125	125	0.63	0.09	1.37
Case 3[a]—Pitch: $B=0.25$ deg, $t_2=10$ ms						
Fourier series	0.064	15.5	17.6	0.25	0.06	1.02
Sinusoidal estimate	0.091	17.6	17.6	0.27	0.05	1.37
Drift and acceleration estimate	0.094	18.5	17.6	0.27	0.05	1.40
Case 4[b]—Pitch: $B=0.486$ deg, $t_2=20$ ms						
Fourier series	0.021	20.4	31.2	0.29	0.23	0.31
Sinusoidal estimate	0.057	31.1	31.1	0.38	0.15	0.63
Drift and acceleration estimate	0.060	33.0	31.1	0.37	0.14	0.66

[a] Parameters not listed are shown in Fig. 1.
[b] $H=0.1$, $\zeta=0.7$, $\omega_n=20$ Hz, $t_1=20$ ms, $\lambda=1$ s, $t_3=10$ ms.

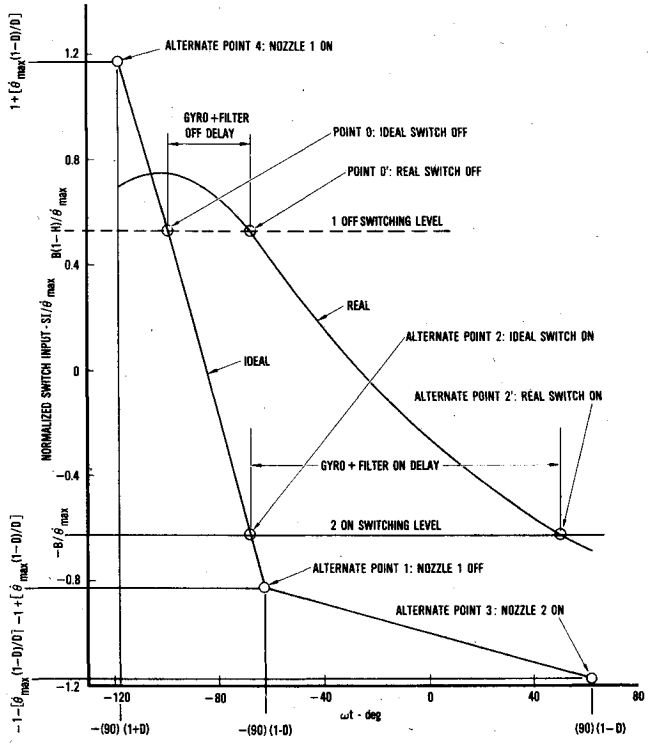

Fig. 3 Switch input.

In Eq. (4), G_n and ϕ_n $(0\leq\phi_n\leq\pi)$ represent the sinusoidal gain and phase lag of the rate gyro, and E_n and ψ_n are the gain and phase shift of the filter at the frequency $n\omega$. In Fig. 3, the line labeled real is case 1 of Table 2 calculated by Eq. (4) using 50 terms. The differences between real and ideal histories of switch input on the switching level lines are graphical displays of the time delays due to the gyro and filter.

Limit Cycle Rate and Duty Fraction

The limit cycle solution is that pair of values of D and $\dot{\theta}_{max}$ for which the same values of t_{off} and t_{on} result from the phase plane Eq. (2), and the time plane Eqs. (3) and (4). The limit cycle frequency and maximum angle are then calculated by Eq. (1). The limit cycle solution can be found by a simple digital computer program, which for each trial pair, D and $\dot{\theta}_{max}$, computes enough of the Fourier series response by Eq. (4) so that the real intersections with the on and off switching levels are found by interpolation. The ideal intersections with the switching levels are found analytically using Eq. (3); then the linear element on and off delays are found from the time differences between the real and ideal intersections. Valve delays are added to obtain t_{on} and t_{off} for the time plane. Phase plane t_{on} and t_{off} are calculated directly by Eq. (2). With D fixed, $\dot{\theta}_{max}$ is decreased by steps, and the values of t_{off} and t_{on} from both sources are compared. When a difference reverses sign, the value of the maximum rate for which t_{off} or t_{on} from the Fourier analysis equals the value of t_{off} or t_{on} from Eq. (2) is calculated by linear interpolation. After the rate for t_{on} equality and for t_{off} equality is found, the program changes duty fraction by one step and repeats the stepping procedure on $\dot{\theta}_{max}$. When the difference between the two rates changes sign the solution values of D and $\dot{\theta}_{max}$ are calculated by interpolation.

Using a program like that outlined above, the four example limit cycles shown in Table 2 were calculated. The limit cycle parameters that result from two commonly used estimates of the linear element delays applied in an inverse form of Eq. (2), are shown for comparison. Neither estimating method is accurate. The duty fraction is overpredicted by 40 to 400%. The sinusoidal delay estimates were made by replacing the half-deadband by B/G, where G is the combined sinusoidal gain factor at the limit cycle frequency. It was assumed that the sum of the sinusoidal lags constitute the on or off delay. The drift and acceleration delays were calculated by assuming that s/ω_n and st_2 are both much less than one. For cases 1 and 2, $st_2\approx 1$; hence, this method is not applicable. By neglecting second and higher powers in small quantities, the approximation that the on delay is the sum of the ramp lags was derived from the transfer functions. The approximate off delay under acceleration is slightly greater.

Acknowledgments

This work was supported by the Space Division of Air Force Systems Command under contract F0-4701-80-C0081.

References

[1] Patapoff, H., "Application of the Rate Diagram Technique to the Analysis and Design of Space Vehicle On-Off Attitude Control Systems," American Rocket Society Guidance, Control and Navigation Conference, Stanford University, Palo Alto, Calif., Aug., 1961.

[2] Graham, D. and McRuer, D., *Analysis of Nonlinear Control Systems*, John Wiley, New York, 1961, pp. 77-143.

[3] Truxal, J. G., *Automatic Feedback Control System Synthesis*, McGraw Hill, New York, 1955, pp. 548-550 and 559-612.